



HAL
open science

Stochastic modelling and prediction of fatigue crack propagation using piecewise-deterministic Markov processes

Anis Ben Abdesslem, Romain Azaïs, Marie Touzet-Cortina, Anne Gégout-Petit, Monique Puiggali

► **To cite this version:**

Anis Ben Abdesslem, Romain Azaïs, Marie Touzet-Cortina, Anne Gégout-Petit, Monique Puiggali. Stochastic modelling and prediction of fatigue crack propagation using piecewise-deterministic Markov processes. 2015. hal-01178988v1

HAL Id: hal-01178988

<https://hal.science/hal-01178988v1>

Preprint submitted on 21 Jul 2015 (v1), last revised 30 Apr 2016 (v2)

HAL is a multi-disciplinary open access archive for the deposit and dissemination of scientific research documents, whether they are published or not. The documents may come from teaching and research institutions in France or abroad, or from public or private research centers.

L'archive ouverte pluridisciplinaire **HAL**, est destinée au dépôt et à la diffusion de documents scientifiques de niveau recherche, publiés ou non, émanant des établissements d'enseignement et de recherche français ou étrangers, des laboratoires publics ou privés.

Stochastic modelling and prediction of fatigue crack propagation using piecewise-deterministic Markov processes

A. Ben Abdesslem[§], R. Azaïs^{†,‡}, M. Touzet-Cortina^{*‡}, A. Gégout-Petit^{†,‡}, and M. Puiggali[§]

[§]Université de Bordeaux, I2M CNRS UMR 5295, France

[†]Inria Nancy-Grand Est, Team BIGS

[‡]Institut Élie Cartan de Lorraine, Université de Lorraine, Nancy, France

[‡]Bordeaux INP, I2M CNRS UMR 5295, France

Abstract

Fatigue crack propagation is a stochastic phenomenon due to the inherent uncertainties originating from material properties, environmental conditions and cyclic mechanical loads. Stochastic processes offer thus an appropriate framework for modelling and predicting crack propagation. In this paper, we propose to model and to predict the fatigue crack growth by a piecewise-deterministic Markov process associated with deterministic crack laws. First, we propose a regime-switching model to express the transition between Paris' regime and rapid propagation which occurs before failure. Both regimes of propagation are governed by a deterministic equation whose parameters are randomly selected in a finite state space. This one has been adjusted from real data available in the literature. The crack growth behaviour is well-captured and the transition between both regimes is well-estimated by a critical stress intensity factor range. The second purpose of our investigation deals with the prediction of the fatigue crack path and its variability based on measurements taken at the beginning of the propagation. We show that our method based on this class of stochastic models associated with an updating method provides a reliable prediction and can be an efficient tool for safety structures in a large variety of engineering applications. In addition, the proposed strategy requires only few information to be effective and is not time-consuming.

Keywords: Fatigue crack propagation, Uncertainties, Stochastic processes, Piecewise-deterministic Markov processes, Regime-switching models, Prediction

1 Introduction

Fatigue crack growth (FCG) in materials exhibits a wide range of scatter even under controlled experimental conditions, see [Virkler et al. \[1979\]](#), [Wu and Ni \[2007\]](#), [Casciati et al. \[2007\]](#), [Moreno et al. \[2003\]](#), [Ghonem and Dore \[1987\]](#). Various sources of scatter exist during the fatigue life, which can be divided into crack initiation and crack growth periods. For each period, the sources of uncertainties may be different. It is well-known that crack initiation, including the first micro-crack growth is a discontinuous process which is dependent on mechanical parameters but also on microstructure and material surface quality (local surface inhomogeneities, small surface irregularities and slight surface damage). In the second period, the crack growth mainly depends on mechanical parameters (applied loads, mechanical properties, etc.). For these reasons, it is technically significant to consider crack initiation and crack growth periods separately. In the present work, our attention is only focused on the crack growth periods.

*Corresponding author; e-mail: marie-benedicte.touzet-cortina@u-bordeaux.fr

Stochastic modelling strategies are relevant to consider the effects of uncertainties. Some papers have addressed the stochastic process framework to model fatigue crack propagation. Indeed, this context enables the introduction of certain variabilities to the typical deterministic laws to describe FCG under constant or variable amplitude fatigue loading, see for instance [Righiniotis and Chryssanthopoulos \[2003\]](#), [Mohanty et al. \[2009\]](#), [Sankararaman et al. \[2011\]](#), [Chang et al. \[1981\]](#), [Xiang and Liu \[2011\]](#), [Zapatero and Domínguez \[1990\]](#), [McMaster and Smith \[2001\]](#), [Wu and Ni \[2003\]](#) and the references therein. Among the deterministic models of FCG proposed in the literature, the Paris-Erdogan and Forman laws, respectively proposed by [Paris and Erdogan \[1963\]](#) and [Forman et al. \[1967\]](#), are widely used because of their simplicity and the limited number of parameters involved. Certain strategies are provided to input randomness into these models and to treat FCG from a stochastic point of view. A popular idea suggested in the literature consists in adding to the deterministic law a multiplicative noise function which is generally a non-negative random process, see for instance [Casciati et al. \[2007\]](#). For example, Gaussian white noise is used by [Sobczyk and Spencer Jr. \[1992\]](#) to add randomness to the deterministic FCG law. Coupled with a filtering technique, this modified law excludes the possibility of negative crack growth rates. The same strategy is followed by [Yang and Manning \[1996\]](#). These authors model the noise function by a stationary lognormal random process with median unity. The strip-yield model included in the NASGRO software developed by [NASA \[2000\]](#) is widely used to simulate crack growth under variable amplitude loading, see for instance [Skorupa et al. \[2007\]](#). More recently, [Beck and de Santana Gomes \[2013\]](#) used the polynomial chaos expansions in combination with the Karhunen-Loève series for accurate and efficient representation of random crack propagation data. They used two different experimental data sets from literature to demonstrate the ability of their model to simulate and predict the fatigue crack propagation.

Markov processes are also proposed to address stochastic modelling of FCG. [Mattrand and Bourinet \[2011\]](#) used Markov chains to propagate the variability affecting non-proportional load sequences. [Dhondt \[1995\]](#) considered discrete Markov methods to handle the uncertainties of initial crack length and loading. [Zou \[2003\]](#) derived a model based on the fracture mechanics theory and the diffusive Markov processes to treat the variabilities affecting material resistance and stress loading. Among the Markov processes suitable to perform crack modelling, one may also consider the class of piecewise-deterministic Markov processes (PDMP's) frequently employed in safety and reliability. These stochastic models have been introduced by [Davis \[1984\]](#) to handle both discrete events (changes of regime or failures in our context) and continuous evolution of physical phenomena (crack length in our context). To the best of our knowledge, [Chiquet et al. \[2009\]](#) were the first authors to use PDMP's to model FCG as a degradation mechanism that continuously evolves in time with the growth rate changing at random times. Among the papers about stochastic models cited above, [Mohanty et al. \[2009\]](#), [Sankararaman et al. \[2011\]](#), [Xiang and Liu \[2011\]](#), [Zapatero and Domínguez \[1990\]](#) propose prediction and validation methods. We also refer the reader to [Guan et al. \[2012\]](#) who propose an inference method based on maximum relative entropy in order to predict the propagation phase of a crack knowing only few points of the beginning of the propagation.

Even if among the aforementioned works, the effects of random loading have been sometimes investigated, we restrict ourselves to the source of uncertainties related to material properties which are observed in large replicate fatigue crack propagation tests. Therefore, we use in this article the data set presented in [Virkler et al. \[1979\]](#) and composed of 62 specimens of 2024-T3 aluminium alloys tested under constant amplitude loading. The aim of this paper is to show the ability of PDMP's to model crack propagation in order to tackle two specific problems: the first one is to capture the transition time between two regimes of propagation and the second one is to predict the behaviour of a crack until the acceleration phase using the first experimental points of its propagation as conditional events.

The objective of the first part of this work is to detect the conditions of crack growth instability that is the transition between the stable region of propagation and the unstable one when the crack growth extends in a rapid manner. In this way, we propose a regime-switching model: we combine two deterministic laws using the more suitable one for each specific period. In the second part, the model is associated with an updating method to predict the whole trajectory of a given crack in order to manage the structure safety using experimental data provided by non-destructive control. FCG is modelled by a PDMP whose deterministic flow is given by either Paris-Erdogan or Forman law. Uncertainties are integrated through the material

parameters of the above-mentioned laws and through the transition time between regimes of propagation.

The layout of the paper is as follows. In Section 2, we expose the model formulation via PDMP's and based on known mechanistic crack growth laws. Section 3 is dedicated to the transition between the two stages of propagation through our model. Section 4 deals with the prediction of crack propagation using PDMP's associated with an updating method. Finally, Section 5 gives some elements of discussion and perspectives.

2 Model formulation

2.1 Definition of PDMP's

Piecewise-deterministic Markov processes form a class of non-diffusion stochastic models introduced in the literature by Davis [1984] in operational research to model physical systems whose dynamics can be disrupted by punctual and random events (non-continuous changes). Consequently, PDMP's are described by two variables: a usual Euclidean state and a discrete variable (called mode or regime) which takes values in a discrete set. In this context, the state variable is representative of the physical system (state, speed, length of a crack, etc.) while the discrete variable reflects the operating mode or a regime of evolution (stage of propagation in our case). It should be noted that the dynamic of the Euclidean variable of a PDMP is governed, between two jumps, by a deterministic differential equation, unlike models often encountered in the literature in which the physical states are assumed to be piecewise-constant or diffusive. The randomness of such a process comes from the jump times and the punctual changes occurring at these times.

More precisely, a PDMP is a two-component process (μ_t, X_t) where the mode μ_t takes its values in a finite state space \mathcal{M} , while X_t represents the physical variable and evolves in an open subset of \mathbb{R} or \mathbb{R}^d . The motion of the continuous part X_t is governed by the flow \mathcal{G} of a deterministic differential equation whose parameters are directed by the mode μ_t . The trajectory of such a process is defined in a very intuitive and iterative way: starting from $(\mu_0, X_0) = (M, x)$, the path is given between times 0 and T_1 by:

$$\mu_t = M \quad \text{and} \quad X_t = \mathcal{G}_M(x, t),$$

where T_1 is the first jump time whose distribution depends on the couple (M, x) . At time T_1 , a jump occurs, and the mode is switched according to a transition matrix that gives the probability from one state to another, and so on. An appropriate selection of the state space and of the main features of the process provide a large variety of stochastic models covering many applications as management of complex systems (see Dufour and Dutuit [2002], Zhang et al. [2014]), modelling of degradation (see de Saporta et al. [2012]) or biology (see Beil et al. [2009]). The mathematical properties and the numerical implementations of these processes are the main topic of many recent publications, see Davis [1984, 1993], de Saporta and Dufour [2012], de Saporta et al. [2010], Brandejsky et al. [2013] and the references therein. In the present paper, we want to favor stochastic models whose differential equations between jumps are known, such as Paris-Erdogan and Forman laws described in the sequel.

2.2 Deterministic crack growth models

For ductile materials, FCG rate can be correlated with the cyclic variation of stress intensity factor. The typical logarithmic plot of da/dN versus ΔK is shown in Figure 1: the curve is divided into 3 regions. In region I, referred to near-threshold region, crack propagation is a discontinuous process which is extremely slow at very lows values of ΔK . In the large and linear region II, a power-law relationship between crack growth rate and stress intensity factor range is observed. Finally, region III corresponds to the increase of crack propagation rate when the stress intensity factor tends to the critical value K_C . Many deterministic laws have been proposed in the literature for modelling the crack behaviour in region II. Among them,

Paris-Erdogan’s law is certainly the most used for steels and aluminium alloys. It was introduced by [Paris and Erdogan \[1963\]](#) and is defined from the following equation:

$$\frac{da}{dN} = C(\Delta K)^m, \quad (1)$$

where da/dN is the crack growth rate per cycle, a is the fatigue crack length, N is the number of cycles, C and m are the Paris’ law parameters and ΔK is the range of the stress intensity factor. In most cases, ΔK is given by the formula:

$$\Delta K = Y(a)\Delta\sigma\sqrt{\pi a}, \quad (2)$$

where $Y(a)$ is a dimensionless factor that considers the crack shape and the geometry of the specimen and $\Delta\sigma = \sigma_{\max} - \sigma_{\min}$ is the stress range.

Even with its popularity and its accuracy in describing the stage II of propagation, the model given by equation (1) is not well-adapted to express the crack growth instability at the beginning of region III. Among the variants of Paris equation developed to overcome this drawback, [Forman et al. \[1967\]](#) suggested a model given by equation (3). This law captures the rapid increasing of growth in region III and includes the stress ratio $R = \sigma_{\min}/\sigma_{\max}$ and the fracture toughness K_C :

$$\frac{da}{dN} = \frac{C(\Delta K)^m}{(1-R)K_C - \Delta K}, \quad (3)$$

where K_C represents the maximal value of the stress intensity factor required to induce failure. In our approach, the fracture toughness K_C is assumed to be fixed and known.

Figure 1 approximately here.

2.3 PDMP’s applied to fatigue crack propagation

PDMP’s are suitable for modelling and predicting degradation processes induced by the presence of cracks in structural components. In particular, the jumps are suitable to express the continuous damage induced by crack propagation. Within this context, [Chiquet et al. \[2009\]](#) consider that FCG changes through small shocks occurring at random times. Precisely, these authors choose to use PDMP’s without any constraint on the number of possible jumps associated with the deterministic Paris’ law. They note that the jump rate is not time-homogeneous since the frequency of jumps increases at the end of the path. Unlike this approach, we assume that crack propagation can be expressed by a simple PDMP with only one jump in order to give a physical meaning to this jump and also to bring some flexibility to the model: we speak about a regime-switching model. In the first case presented in Section 3, the jump can express the transition between two regimes of propagation when two distinct laws are used before and after the jump. In this case, the deterministic flow \mathcal{G} driving the propagation between two jumps is given by either the differential equation (1) in the first part or equation (3) in the second part. We will see in Section 4 that this idea may also give some flexibility to a model of propagation based on a unique law. Indeed, the differential equation \mathcal{G} driving the propagation will always be given by equation (1) but its parameters will change at the jump time. The main ideas for the construction of our model are given in the sequel.

- We choose two laws of propagation \mathcal{G}_{M_1} and \mathcal{G}_{M_2} among equations (1) and (3). Both equations depend on a two-dimensional parameter (m, C) .
- At time 0, (m_1, C_1) is randomly selected in a finite state space \mathcal{M} , and FCG deterministically evolves according to the deterministic equation of propagation given \mathcal{G}_{M_1} with $(m, C) = (m_1, C_1)$ until a random time denoted by T . Next, new parameters (m_2, C_2) are selected according to a Markov transition on \mathcal{M} : after T , the process follows the equation \mathcal{G}_{M_2} with parameters (m_2, C_2) .

The model is thus defined from the following features:

- The two equations of propagation \mathcal{G}_{M_1} and \mathcal{G}_{M_2} . It should be noted that they can be obtained from the same mechanistic law.
- The initial distribution of (m_1, C_1) , the parameters of \mathcal{G}_{M_1} , given by a probability distribution on \mathcal{M} .
- The law of the jump time depending on the parameters (m_1, C_1) .
- The law of transition between the parameters of the first regime (m_1, C_1) and the second one (m_2, C_2) . This transition is defined from a stochastic matrix on \mathcal{M} .

3 Transition of FCG between stage II and stage III

In this section, we use PDMP's introduced in the previous section in order to investigate the transition between regions II and III of propagation. We consider Paris equation (1) for the crack growth propagation \mathcal{G}_{M_1} corresponding to region II and Forman law (3) for \mathcal{G}_{M_2} corresponding to the rapid crack propagation in region III. T is the random time of jump between both regimes. We fit experimental data provided by Virkler et al. [1979] to theoretical curves issued from the model and we obtain a set of parameters that is statistically analysed.

3.1 Experimental data

Virkler et al. [1979] tested 62 identical centre-cracked aluminium alloy specimens (152 mm wide and 2.54 mm thick) under constant amplitude loading $\Delta\sigma = 48.28$ MPa at a stress ratio $R = 0.2$. The number of loading cycles for the crack tip to advance a predetermined increment Δa was recorded from an initial crack length of 9 mm to a final length of 49.8 mm. 68 crack growth histories were obtained from these tests. For each crack and each measurement $1 \leq i \leq 164$, a^i denotes the crack length after N^i loading cycles. These quantities represent the empirical data required to build the proposed modelling. The 68 experimental crack length curves versus the number of cycles are presented in Figure 2. A large scatter is obtained which corresponds to the variability of the crack growth process. The logarithmic representation of the crack growth rate in terms of ΔK is also presented in Figure 3. As it was schematized in Figure 1, we observe a linear increase of da/dN on the largest part of the propagation with some changes at the end and to a lesser extent, at the beginning.

Figures 2 and 3 approximately here.

3.2 Fit of experimental curves

This section is devoted to the determination, for each experimental curve, of the nearest theoretical curve coming from the model. We tackle this problem with an optimisation formulation. By definition of our model, a theoretical curve is determined by five parameters (m_1, C_1, T, m_2, C_2) with (m_1, C_1) the Paris law parameters, (m_2, C_2) the Forman law parameters and T the jump time. Thus, to properly fit each experimental curve to a theoretical one, we must determine the optimal parameters $(m_1^*, C_1^*, T^*, m_2^*, C_2^*)$ that minimise an objective function. The latter measures the distance between crack lengths given by the experimental curve and by the theoretical one obtained by discretisation of deterministic laws. The optimisation problem can be stated as follows:

$$\underset{(m_1, C_1, T, m_2, C_2)}{\text{Minimise}} \quad f(m_1, C_1, T, m_2, C_2) = \sum_{i=1}^{164} [a_{\text{theo}}^i(m_1, C_1, T, m_2, C_2) - a_{\text{exp}}^i]^2, \quad (4)$$

where a_{theo}^i and a_{exp}^i are theoretical and experimental crack lengths at each measurement i , respectively. The authors would like to emphasise that this optimisation problem is far to be obvious. Initially, the values assigned to the material parameters are randomly selected from the range of values, and we use a simulated annealing algorithm to solve the above optimisation problem. A metaheuristic algorithm is justified by its ability to determine the global optimum even in this highly non-convex context. The reader can find further information about the implementation of simulated annealing algorithms and parameter selection in [Fabian \[1997\]](#), [Dréo \[2006\]](#).

3.3 Results

We first focus on the quality of the fitting. Figure 4 displays the graphs of the worst (left) and the best (right) fitted versions of the experimental curves among the 68's. In each case, the model fits very well the crack length evolution. We can also point out that the end of crack propagation is accurately described by our regime-switching model using Forman's law for the transition between stage II and stage III. We can establish a connection between this result and the comment of [Chiquet et al. \[2009\]](#) already presented in Subsection 2.3. Actually they notice that, in their model, the number of jumps increases at the end of the propagation. According to us, this result is due to the rapid increase of the crack propagation related to the beginning of crack growth instability which is characterized, in our case, by the switching to a more appropriate law.

Figure 4 approximately here.

Relationships between m and $\log(C)$ for each regime are presented in Figure 5. The values of the coefficient of multiple correlation R^2 for both Paris and Forman laws demonstrate the accuracy of the linear model between these parameters. This correlation between m and $\log(C)$, already known in the literature for propagation with only one regime (see [Cortie \[1991\]](#), [Bergner and Zouhar \[2000\]](#), [Carpinteri and Paggi \[2007\]](#)) is again observed in both regimes of our model. According to [Carpinteri and Paggi \[2007\]](#), the correlation between Paris parameters m and $\log(C)$ is due to the fact that the transition from Paris' regime (region II) to region III coincides with the Griffith-Irwin theory of instability. On the other hand, [Bergner and Zouhar \[2000\]](#) stated that the high correlation between m and $\log(C)$ is only due to the logarithmic representation. Let us note that, since the relationship between parameters is found for both regimes with Paris and Forman laws, we suppose that the correlation is only formal without real physical relevance. However, this linear relationship between m and $\log(C)$ in each region is very useful to our model of PDMP: indeed, we will take advantage of it in Section 4 below.

Figure 5 approximately here.

3.4 Statistical analysis of the transition times

We focus on the crack length, the number of cycles and the stress intensity factor range ΔK values at the estimated transition time T^* . Their statistical characteristics are listed in Table 1. As expected, the jump associated to the transition between Paris and Forman laws occurs at the end of the propagation. The mean value of ΔK is equal to $20.8 \text{ MPa}\sqrt{m}$ and corresponds to the end of the linear part of the $\log(da/dN)$ versus $\log(\Delta K)$ curve (see Figure 3) obtained for $\Delta K = 21 \text{ MPa}\sqrt{m}$. If we assume that the crack instability condition is reached for $K_{\text{max}} = K_C$ at the transition between stage II and stage III, the corresponding stress intensity factor is given by:

$$\Delta K = K_{\text{max}} - K_{\text{min}} = (1 - R)K_C, \quad (5)$$

where $R = K_{\text{min}}/K_{\text{max}} = 0.2$. Mean, maximal and minimal values of fracture toughness K_C connected with ΔK values obtained from the above equation are presented in Table 1. We remark that K_C values

are contained between 20 and 32 MPa \sqrt{m} . In handbooks of [ASM International \[1990, 1996\]](#), minimal and maximal values for fracture toughness determined experimentally for the 2024-T3 aluminium alloy are equal to 15 MPa \sqrt{m} and 50 MPa \sqrt{m} , respectively. There is a good agreement between estimated values obtained in our investigation and lower values recorded in handbooks. This result means that the choice of PDMP with only one jump combined with appropriate deterministic laws gives results with significant physical relevance in terms of ΔK . This quantity itself is deterministically related to the length of the cracks through equation (2). The knowledge of such a critical crack length is very important for safety of structures and may be used as a criterion for a designer to avoid sudden failures.

| | Mean | Standard deviation | Minimum | Maximum |
|---|--------|--------------------|---------|---------|
| Crack length (mm) | 39.53 | 4.55 | 30.40 | 48.20 |
| Transition times (number of cycles) | 241401 | 19184 | 192389 | 296091 |
| ΔK (MPa \sqrt{m}) | 20.8 | 1.0544 | 16.5 | 25.3 |
| K_C (MPa \sqrt{m}) from equation (5) | 25.8 | NA | 20.6 | 32 |

Table 1: Statistics concerning the crack length at the jump time, the transition time and the corresponding stress intensity factor range.

4 Prediction of fatigue crack propagation

The purpose of this part is to predict the whole trajectory of FCG using a PDMP model and the knowledge of a few inspections performed at the beginning of the propagation. From a mathematical point of view, it consists in predicting the crack behaviour knowing only the first points of its curve. The principle of the updating method is the following: we construct a suitable model of crack propagation and then, the knowledge of the beginning of propagation of a given crack allows us to reduce the possible paths inside the model, these paths leading to the future of this given crack. We present first the dynamic model and the updating method, then we analyse the quality of the prediction for the whole trajectory (phases II and III) of each crack of the Virkler dataset.

4.1 Calibration of the model

We consider a PDMP for modelling the crack propagation, but here we strongly use some measurements taken at the beginning of the propagation. As a consequence, Forman’s law, very suitable to detect crack growth acceleration, is not well-adapted in this new context. For this reason, we propose a model only based on the Paris’ law both before and after the jump time at which only material parameters m and C change. In the framework of Subsection 2.3, we model crack propagation as follows: crack growth rate is first driven by Paris equation (1) with a set of parameters and at a random time, the set of parameters related to Paris dynamic changes. To avoid any confusion with the previous work presented in Subsection 2.3, this new model is called Paris model with one jump. Randomness comes again from three sources: the stochastic choice of parameters at the beginning denoted by (m_1, C_1) , the random jump time T and the random transition between parameters (m_1, C_1) and (m_2, C_2) . Nevertheless, we would like to emphasise that the aim of this second investigation is to provide a simulation model suitable to predict FCG, while the goal of the previous part was to capture the transition between regimes II and III of the propagation.

Let us recall that the features of a PDMP for crack propagation are the finite state space \mathcal{M} for the material parameters (m, C) , their initial distribution, their transition matrix and finally the distribution of the jump time. The last three govern the randomness of our simulation model and will be estimated by their empirical version, while the choice of the state space is quite less crucial. First of all, we mimic Subsection 3.2 and more precisely equation (4) to fit each experimental curve to a theoretical one issued from the Paris

model with one jump. These new data $(m_1^*, C_1^*, T^*, m_2^*, C_2^*)$ are used to fit the features of our simulation model:

- Finite state space \mathcal{M} for the parameters (m, C)
We group the 68 values of m_1^* in p classes and we propose the centers of these classes as a first set of points for m . Then we use the linear link between m and $\log(C)$ to propose two corresponding values of C at each class center m , that is $\log(C) = a + bm + \sigma$ and $\log(C) = a + bm - \sigma$ where a , b and σ have been estimated from the linear regression between m_1^* and $\log(C_1^*)$. Now we have a first set of $2p$ pairs of (m, C) corresponding to the first regime of prediction for the given crack. A second set of points for \mathcal{M} is chosen using the fitted law of $\log(C_1^*) - \log(C_2^*)$ (Gaussian in our case) and again from the linear correlation between m_2^* and $\log(C_2^*)$. The final set \mathcal{M} thus contains $4p$ pairs (m, C) .
- Initial distribution of parameters (m, C)
The initial law of these parameters is given by a probability law on \mathcal{M} obtained as the empirical distribution of the 68 values of m_1^* on the classes obtained at the previous step.
- Jump time distribution
The jump time law depends on the parameters (m, C) . As explained below, this law is almost not used in the prediction, because we force the jump to occur before the last observed point of propagation. Thus, we simply use an exponential variable with constant coefficient estimated by maximum likelihood in each mode of (m, C) .
- Transition distribution of parameters (m, C)
The transition law between parameters (m_1, C_1) and (m_2, C_2) is given by a transition matrix on \mathcal{M} obtained from the empirical conditional distribution of the 68 values of (m_1^*, C_1^*) and (m_2^*, C_2^*) on the classes build at the first step.

Figure 6 shows a set of simulated curves from $p = 1$. It should be noted that in this case there are only 4 possible values for parameters m and C in \mathcal{M} . We see that even if we have two possible curves at the beginning of the propagation, and only two propagation regimes after the jump time T , the bundle is rich because of the diversity of jump times. We can note that the simulated bundle includes the experimental one (see Figure 2). It is also interesting to choose $p > 1$ in the purpose of prediction. This is the object of the next section.

Figure 6 approximately here.

4.2 Updating method

We follow here an idea developed by Perrin [2008] and Guan et al. [2012]. The assumption of the updating method is to use the information of the first points of the propagation of a given crack in order to reduce the number of possible trajectories of the model: it means that the set of parameters (m, C) in \mathcal{M} is reduced to predict the future of the propagation. It leads to a thin and precise bundle of crack path. Suppose that we have ℓ measures from an experimental curve. The Paris model contains $2p$ theoretical curves corresponding to $2p$ values of (m, C) for the first part of the propagation. For a given experimental curve, from ℓ points of measure, it is easy to compute the distance to each of the $2p$ theoretical curves defined by the model for the beginning of the propagation with:

$$f(m, C) = \sum_{i=1}^{\ell} [a_{\text{theo}}^i(m, C) - a_{\text{exp}}^i]^2.$$

We proceed in two steps:

Step 1. We compute the $2p$ values $f(m, C)$, $(m, C) \in \mathcal{M}$, in order to choose the r ($r < 2p$) nearest curves among the $2p$ theoretical curves of the model. Figure 7 (top) summarizes this procedure for $p = 5$ and $r = 4$: the experimental measurements are drawn with black points and we choose here the 4 nearest theoretical curves (solid lines) among the $2p = 10$ possible paths.

Step 2. We work with each of the r possible trajectories chosen at the first step and corresponding to r values of (m, C) . For a given crack and each number of cycles N^i corresponding to the point of measure a_{exp}^i , we draw the $2p$ possible paths starting from the point $(N^i, a_{\text{theo}}^i(m, C))$ and compute the distance to the second part of the experimental curve. Again we choose the r nearest among the $2p$ possible paths. This step is illustrated in Figure 7 (bottom) for the jump time at the third measure with $p = 5$ and $r = 4$.

Figure 7 approximately here.

4.3 Validation and results

Unlike Guan et al. [2012] who performed their simulation study only on some specific cracks and until 250 000 cycles, we propose to predict the whole trajectory of all cracks. In order to tackle the versatility of our updating procedure, we propose a leave-one-out method. Indeed, for each experimental crack, we compute the parameters of the Paris model with the 67 remaining cracks. From the ℓ first points of propagation of the involved crack, the obtained model is used to simulate a prediction bundle until the final length 49.8 mm (corresponding to a final number of cycles between 222 000 and 321 000 cycles according to the crack) and we study the quality of the prediction with the following criterion: we compute the distance between the crack and its prediction bundle. This quantity equals 0 if and only if the crack remains inside the bundle along the propagation. More precisely, we determine for each measurement a_{exp}^i , $\ell \leq i \leq 164$, the simulated curve of the prediction bundle which reaches first the size a_{exp}^i , and we denote ν_{min}^i the corresponding number of cycles. We also determine the curve that reaches this size at last and ν_{max}^i stands for the corresponding number of cycles. The quantity d^i denotes the distance between the experimental curve and its prediction bundle at measure i and is defined by:

$$\begin{aligned} d^i &= 0 && \text{if } \nu_{\text{min}}^i \leq N^i \leq \nu_{\text{max}}^i, \\ d^i &= \nu_{\text{min}}^i - N^i && \text{if } N^i \leq \nu_{\text{min}}^i, \\ d^i &= N^i - \nu_{\text{max}}^i && \text{if } \nu_{\text{max}}^i \leq N^i. \end{aligned}$$

Let us remark that the couples $(\nu_{\text{min}}^i, a_{\text{exp}}^i)$ and $(\nu_{\text{max}}^i, a_{\text{exp}}^i)$ define the extreme curves of the prediction bundle. The overall distance between the experimental curve and its prediction bundle is the sum of these local distances normalised by the total number of cycles N^{164} used to reach the final length 49.8 mm, that is:

$$D = \frac{1}{N^{164}} \sum_{i=\ell+1}^{164} d^i.$$

We focus on the results of the leave-one-out method using the model with $p = 5$, that is to say from 20 possible sets of parameters. We distinguish three different crack behaviours according to the number of cycles reached after 160 measurements (end of propagation). Cracks are considered rapid for $N^{160} < 240\,000$ cycles, while they are slow for $N^{160} > 280\,000$ cycles, and thus average for $240\,000 < N^{160} < 280\,000$ cycles. Figure 8 presents three experimental curves with their predicted bundle for two rapid cracks and a slow one. The normalised distance values D defined earlier are calculated for both cracks. For the rapid crack, the experimental curve is always located in the bundle ($D = 0$) or goes out only during a short time around 125 000 cycles ($D \simeq 0.2$). For the slow crack, the experimental curve, is not well-predicted and the corresponding value of D is about 11.6. In this case, the real crack path is discontinuous and presents irregularities due to local microstructural variations characterised by the stop or the slowing down of the crack. However, in this case, the bundle is slightly situated above the experimental curve showing that, in

terms of prediction, the model overestimates the real crack behaviour. Overall results of the cross validation are presented in Table 2. The quantity d^{160} indicates if the crack is in the bundle at the end of its propagation. We obtain that 38% of the experimental curves remain inside the bundle along the propagation ($D = 0$), 72% are at a very low distance ($0 < D < 1$), and two among three are inside the bundle at the end of the propagation ($d^{160} = 0$). Furthermore, we note that all the rapid cracks are well-forecasted ($0 < D < 1$), while any slow crack is accurately simulated ($D > 1$). For slow and some average cracks, the path is not always well-predicted but, in these cases, the bundle is always located above the experimental curve. This means that, in this situation, the model always overestimates the real crack behaviour and that the prediction reduces systematically the risk of rupture. On the contrary, the prediction carried out for rapid cracks and for a large number of average cracks, which appear as the most dangerous situations, is very powerful.

| | Rapid cracks | Average cracks | Slow cracks |
|---------------|--------------|----------------|-------------|
| Occurrences | 11 | 50 | 7 |
| $D = 0$ | 8 | 18 | 0 |
| $0 < D < 1$ | 11 | 38 | 0 |
| $D > 1$ | 0 | 12 | 7 |
| $d^{160} = 0$ | 9 | 35 | 1 |

Table 2: Normalised distance D and crack location at the end of the propagation d^{160} for the different types of crack.

Figure 8 approximately here.

5 Conclusion

We have shown the ability of a simple model of PDMP to address specific problems of fatigue crack propagation. Virkler data have been used in order to confirm the efficiency of our model. In the first part of the paper, we have investigated the advantage to use a switching model with two adapted deterministic laws to capture the change between region II and region III where the crack growth instability occurs. We emphasised that the linear relationship between the material parameters m and $\log(C)$ exists in both regimes of propagation. We showed that the transition can be precisely estimated in terms of stress intensity factor. In addition, the mean stress intensity factor range resulting from the model is very close to the minimal fracture toughness proposed in handbooks for the 2024-T3 aluminium alloy. The idea developed in this paper could be extended to the modelling of the transition between region I and region II by using specific deterministic propagation laws for small cracks. The second problem investigated in this article deals with the crack path prediction using few information at the beginning of the propagation. In practice, the length evolution of a crack found in structural components subjected to cyclic loading can be obtained when structures are periodically inspected with non-destructive technics (NDT). We have shown that the PDMP model combined with an efficient updating method is able to predict the FCG until the rapid crack propagation regime. The dynamic character of the model is suitable for this task probably because it takes into account the acceleration phase. The proposed study has stated the potentiality of the PDMP model to predict crack propagation based on the knowledge of some information which may be issued from NDT. When new measurements become available, we can incorporate them to update the prediction of the remaining life for the structure. Finally, the proposed approach can obviously be extended and generalised to other materials and structures.

Acknowledgements

This work was supported by ARPEGE program of the French National Agency of Research (ANR), project “FAUTOCOES” number ANR-09-SEGI-004.

References

- ASM International. *Properties and Selection: Nonferrous Alloys and Special-purpose Materials*. ASM Handbook. ASM International, 1990.
- ASM International. *Fatigue and fracture*, volume 19 of *ASM Handbook*. ASM International, 1996.
- R. Azais, C. Elegbede, A. Gégout-Petit, and M. Touzet. Estimation, simulation et prévision d'un modèle de propagation de fissures par des processus markoviens déterministes par morceaux. In *Proceedings of $\lambda\mu 17$, La Rochelle, France*, 2010.
- A.T. Beck and W.J. de Santana Gomes. Stochastic fracture mechanics using polynomial chaos. *Probabilistic Engineering Mechanics*, 34:26–39, 2013.
- M. Beil, S. Luck, F. Fleischer, S. Portet, W. Arendt, and V. Schmidt. Simulating the formation of keratin filament networks by a piecewise-deterministic markov process. *J Theo Biology*, 256:518–32, 2009.
- F. Bergner and G. Zouhar. A new approach to the correlation between the coefficient and the exponent in the power law equation of fatigue crack growth. *International Journal of Fatigue*, 22:229–39, 2000.
- A. Brandejsky, B. de Saporta, and F. Dufour. Optimal stopping for partially observed piecewise-deterministic markov processes. *Stochastic Processes and their Applications*, 123(8):3201–3238, 2013.
- A. Carpinteri and M. Paggi. Are the paris' law parameters dependent on each other? *Frattura ed Integrità Strutturale*, 2:10–16, 2007.
- F. Casciati, P. Colombi, and L. Faravelli. Inherent variability of an experimental crack growth curve. *Structural Safety*, 29(1):66 – 76, 2007.
- J.B. Chang, C.M. Hudson, and ASTM Subcommittee E24.06 on Fracture Mechanics Applications. *Methods and Models for Predicting Fatigue Crack Growth Under Random Loading*. A.S.T.M. STP. ASTM, 1981.
- J. Chiquet, N. Limnios, and M. Eid. Piecewise deterministic markov processes applied to fatigue crack growth modelling. *Journal of Statistical Planning and Inference*, 139(5):1657 – 1667, 2009.
- M. B. Cortie. The irrepressible relationship between the paris law parameters. *Engineering Fracture Mechanics*, 40(3):681 – 682, 1991.
- M.H.A. Davis. Piecewise-deterministic markov-processes - a general-class of non-diffusion stochastic-models. *Journal Of The Royal Statistical Society Series B-Methodological*, 46(3):353–388, 1984.
- M.H.A. Davis. *Markov models and optimization*, volume 49 of *Monographs on Statistics and Applied Probability*. Chapman & Hall, London, 1993. ISBN 0-412-31410-X.
- B. de Saporta and F. Dufour. Numerical method for impulse control of piecewise deterministic markov processes. *Automatica*, 48(5):779–793, 2012.
- B. de Saporta, F. Dufour, and K. Gonzalez. Numerical method for optimal stopping of piecewise deterministic markov processes. *Ann. Appl. Probab.*, 20(5):1607–1637, 10 2010.
- B. de Saporta, F. Dufour, H. Zhang, and C. Elegbede. Optimal stopping for the predictive maintenance of a structure subject to corrosion. *Journal of Risk and Reliability*, 226 (2):169–181, 2012.
- G. Dhondt. Application of the discrete markov method to crack propagation problems. *Int J Engng Sci*, 33 (4):457 – 467, 1995.
- J. Dréo. *Metaheuristics for Hard Optimization: Methods and Case Studies*. Springer, 2006. ISBN 9783540230229.

- F. Dufour and Y. Dutuit. Dynamic reliability: A new model. In *Proceedings of $\lambda\mu 13$ -ESREL02, Lyon, France*, 2002.
- V. Fabian. Simulated annealing simulated. *Computers & Mathematics with Applications*, 33(1–2):81 – 94, 1997.
- R. Forman, V. Keary, and R. Eagle. Numerical analysis of crack propagation in cyclic-loaded structures. *Trans ASME J Basic Engng*, 89(3):459 – 464, 1967.
- H. Ghonem and S. Dore. Experimental study of the constant-probability crack growth curves under constant amplitude loading. *Engineering Fracture Mechanics*, 27(1):1 – 25, 1987.
- X. Guan, A. Giffin, R. Jha, and Y. Liu. Maximum relative entropy-based probabilistic inference in fatigue crack damage prognostics. *Probabilistic Engineering Mechanics*, 29:157 – 166, 2012.
- C. Mattrand and J.-M. Bourinet. Random load sequences and stochastic crack growth based on measured load data. *Engineering Fracture Mechanics*, 78(17):3030–3048, 2011.
- F.J. McMaster and D.J. Smith. Predictions of fatigue crack growth in aluminium alloy 2024-t351 using constraint factors. *International Journal of Fatigue*, 23:93 – 101, 2001.
- J.R. Mohanty, B.B. Verma, and P.K. Ray. Prediction of fatigue crack growth and residual life using an exponential model: Part i (constant amplitude loading). *International Journal of Fatigue*, 31(3):418 – 424, 2009.
- B. Moreno, J. Zapatero, and J. Domínguez. An experimental analysis of fatigue crack growth under random loading. *International Journal of Fatigue*, 25(7):597 – 608, 2003.
- NASA. *Fatigue crack growth computer program NASGRO Version 3.0–Reference manual*. JSC-22267B, NASA, Lyndon B. Johnson Space Center, Texas, 2000.
- P.C. Paris and F. Erdogan. A critical analysis of crack propagation laws. *J Basic Engng*, 85(4):528 – 533, 1963.
- F. Perrin. *Prise en compte des données expérimentales dans les modèles probabilistes pour la prévision de la durée de vie des structures*. PhD thesis, Université Blaise Pascal Clermont-Ferrand II, France, 2008.
- T.D. Righiniotis and M.K. Chryssanthopoulos. Probabilistic fatigue analysis under constant amplitude loading. *Journal of Constructional Steel Research*, 59(7):867 – 886, 2003.
- Shankar Sankararaman, You Ling, and Sankaran Mahadevan. Uncertainty quantification and model validation of fatigue crack growth prediction. *Engineering Fracture Mechanics*, 78(7):1487 – 1504, 2011.
- M. Skorupa, T. Machniewicz, J. Schijve, and A. Skorupa. Application of the strip-yield model from the nasgro software to predict fatigue crack growth in aluminium alloys under constant and variable amplitude loading. *Engineering Fracture Mechanics*, 74(3):291 – 313, 2007.
- K. Sobczyk and B.F. Spencer Jr. Introduction: From data to theory. In K. Sobczyk B.F. Spencer, editor, *Random Fatigue*, pages 1 – 7. Academic Press, San Diego, 1992.
- D. Virkler, B. Hillberry, and P. Goel. The statistical nature of fatigue crack propagation. *J Engng Mater Technol*, 101(2):148 – 153, 1979.
- W.F. Wu and C.C. Ni. A study of stochastic fatigue crack growth modeling through experimental data. *Probabilistic Engineering Mechanics*, 18:107 – 118, 2003.
- W.F. Wu and C.C. Ni. Statistical aspects of some fatigue crack growth data. *Engineering Fracture Mechanics*, 74(18):2952 – 2963, 2007. Reliability - Statistical Methods in Fracture and Fatigue.

- Yibing Xiang and Yongming Liu. Application of inverse first-order reliability method for probabilistic fatigue life prediction. *Probabilistic Engineering Mechanics*, 26(2):148 – 156, 2011.
- J.N. Yang and S.D. Manning. A simple second order approximation for stochastic crack growth analysis. *Engineering Fracture Mechanics*, 53(5):677–686, 1996.
- J. Zapatero and J. Domínguez. A statistical approach to fatigue life predictions under random loading. *International Journal of Fatigue*, 12:107 – 114, 1990.
- H. Zhang, F. Innal, F. Dufour, and Y. Dutuit. Piecewise deterministic markov processes based approach applied to an offshore oil production system. *Rel. Eng. & Sys. Safety*, 126:126 – 134, 2014.
- X.L. Zou. Statistical moments of fatigue crack growth under random loading. *Theoretical and Applied Fracture Mechanics*, 39(1):1–5, 2003.

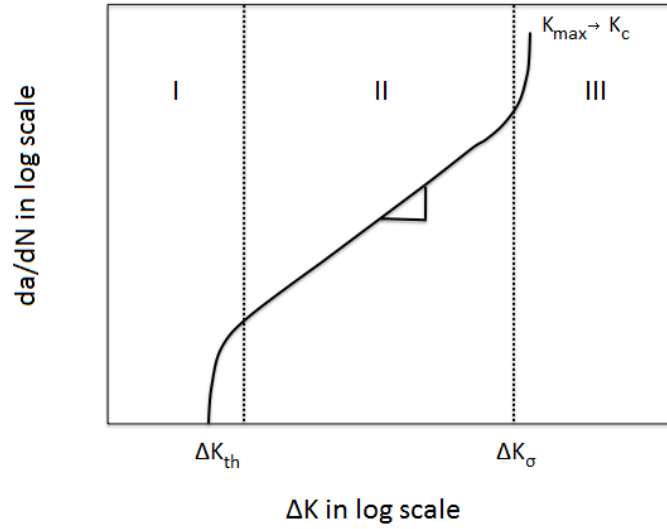


Figure 1: Schematic illustration of the different regimes of fatigue crack propagation. The vertical dashed lines indicate the transition between crack propagation regimes.

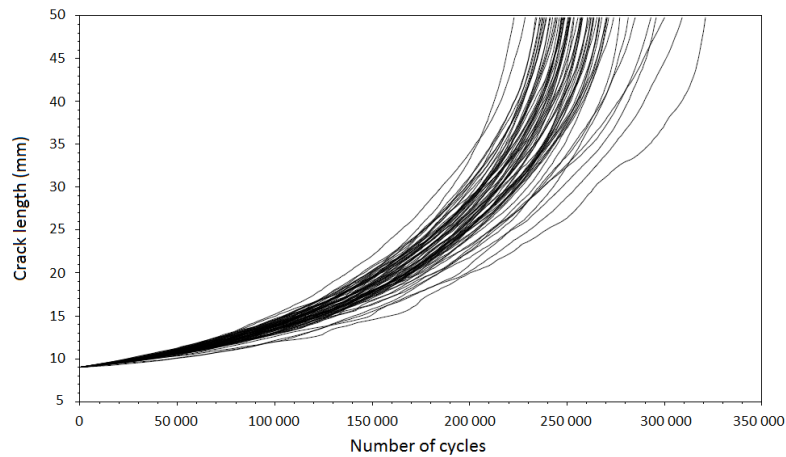


Figure 2: Crack length versus number of cycles for the 68 experiments provided in [Virkler et al. \[1979\]](#).

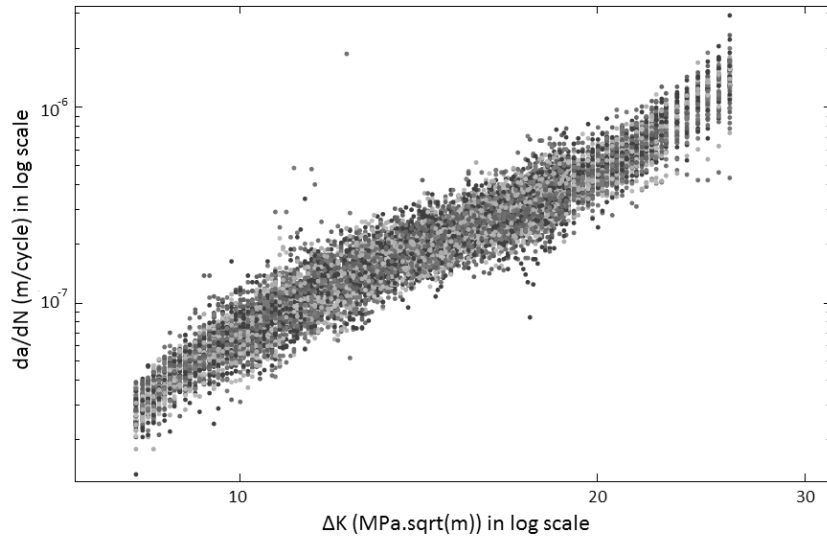


Figure 3: Crack growth rate in terms of ΔK computed from the 68 experiments provided in [Virkler et al. \[1979\]](#).

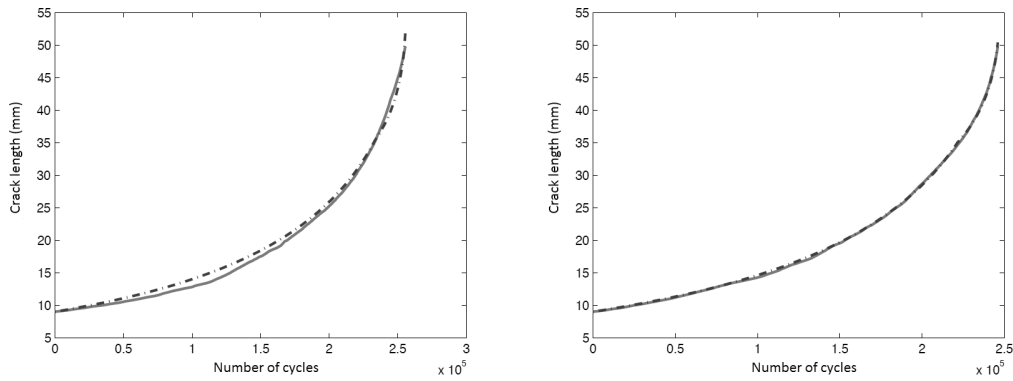


Figure 4: Experimental (solid line) and theoretical (dashed line) curves for the worst (left) and the best (right) fitted propagation length curves.

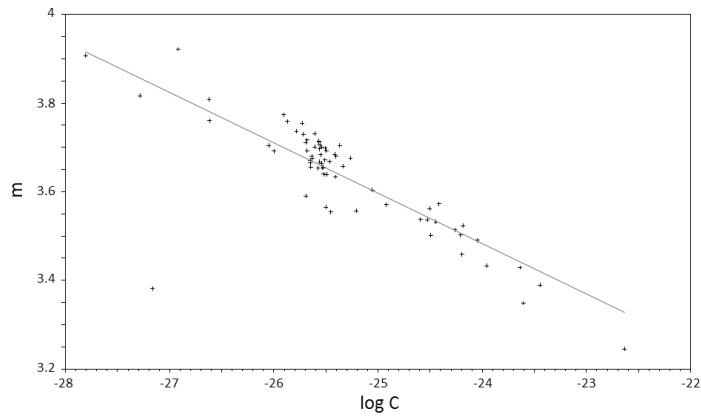
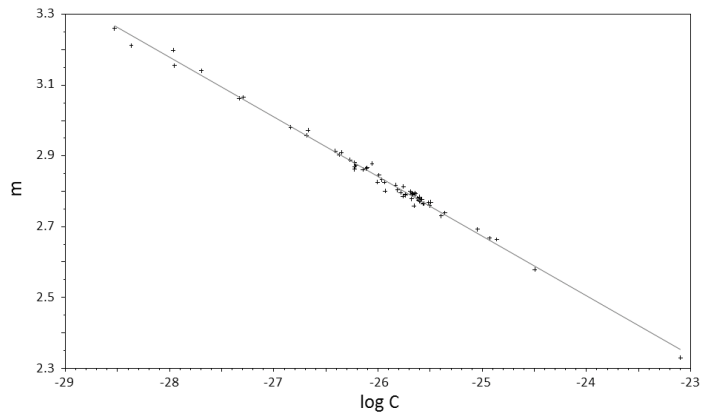


Figure 5: Linear relationship between the material parameters m and $\log(C)$ in the Paris-Forman fitting in the first (top, $R^2 = 0.997$) and second (bottom, $R^2 = 0.819$) regimes.

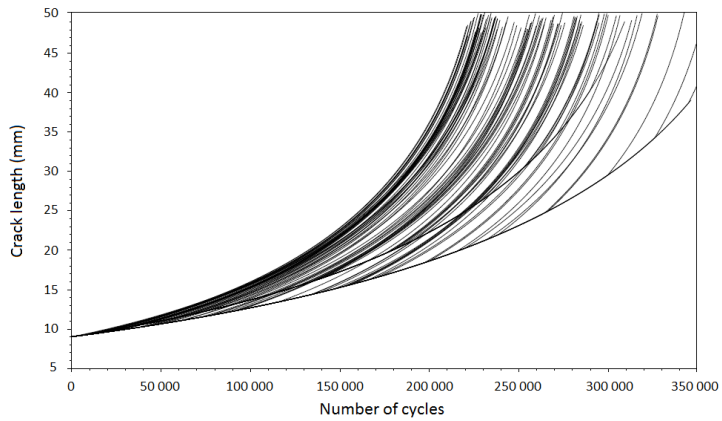


Figure 6: Simulation of crack propagation curves from parameter $p = 1$.

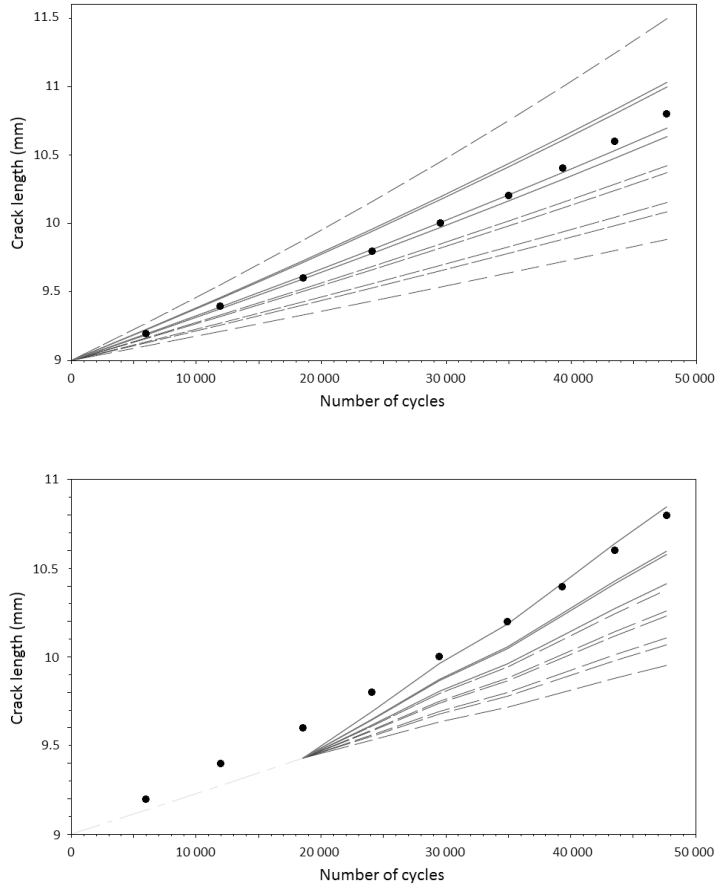


Figure 7: First (top) and second (bottom) steps of the updating method. Experimental measurements ($\ell = 10$) are drawn with black points and solid lines indicate the $r = 4$ nearest theoretical curves among the $2p = 10$ possible paths.

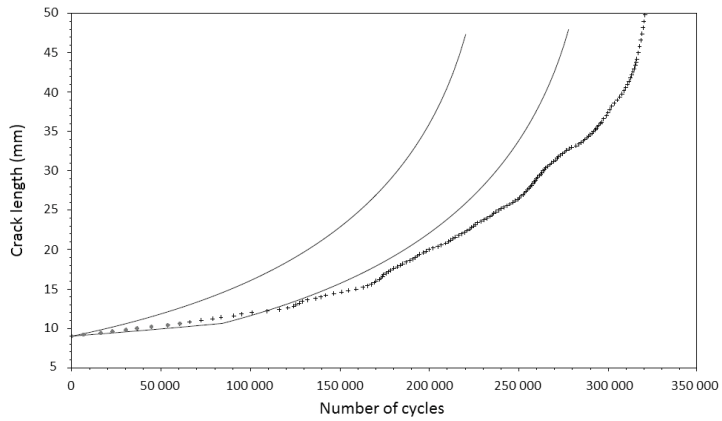
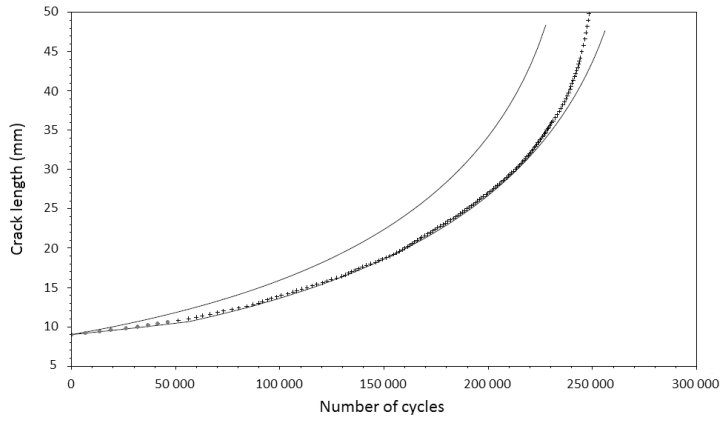
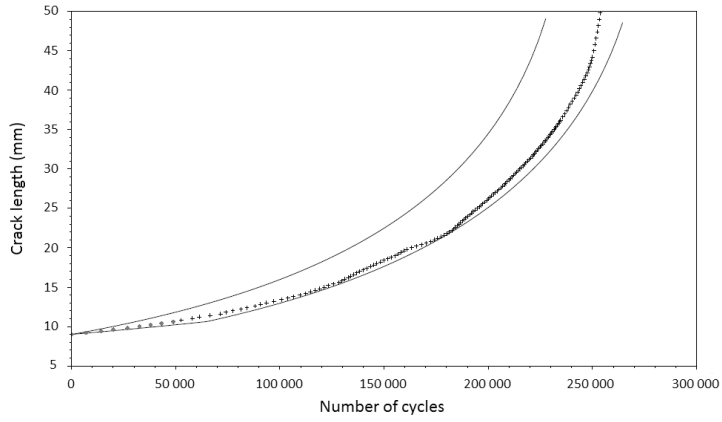


Figure 8: Three experimental propagations with the extreme curves of their prediction bundle obtained from the $\ell = 10$ first measures: rapid cracks with $D = 0$ and $D = 0.2$ and slow crack with $D = 11.6$ (from top to bottom).